Electronic structure and interatomic bonding of crystalline β-BaB_2O_4 with comparison to LiB_3O_5

Yong-Nian Xu and W. Y. Ching
Department of Physics, University of Missouri–Kansas City, Kansas City, Missouri 64110

R. H. French
E. I. Dupont de Nemours and Company, Inc., Central Research and Development Department, E356/323 Experimental Station, Wilmington, Delaware 19880

(Received 12 July 1993)

The electronic structure and the linear-optical properties of the nonlinear-optical crystal β-BaB_2O_4 (BBO) have been calculated using a first-principles band-structure method with the local-density approximation. The results are compared with those of another nonlinear-optical crystal LiB_3O_5 (LBO). An indirect band gap of 5.52 eV and a direct gap of 5.61 eV at Γ for BBO are obtained, which are to be compared with the measured optical gap of 6.43 eV. It is shown that the electronic structure of the BBO is dominated by the characteristic ionic $(B_3O_6)^{-3}$ group in which the two different O sites show markedly different bonding structures. Comparison of charge-density distributions in BBO and LBO shows that the ionic groups are linked together in forming a networklike structure. The Ba atom in the BBO crystal is found to be bonded to the O ions in the adjacent layers in a partly covalent, partly ionic manner due to the presence of large semi-core-like $5p$ orbitals. The calculated optical properties for both BBO and LBO crystals are in good agreement with the measured vacuum ultraviolet spectrum especially in the region of absorption threshold. The agreements between theory and experiment near the absorption edges are much closer than that reflected by the gap values alone.

I. INTRODUCTION

In the late 1970s, Chen proposed an anionic-group theory to describe the nonlinear-optical susceptibilities of borate crystals.[1] The theory asserts that the second-harmonic generation (SHG) of a nonlinear inorganic crystal can be considered as the superposition of anion groups in the crystal which can be estimated from quantum molecular calculations. Subsequently, Chen and coworkers succeeded in growing many new inorganic crystals in the borate family with excellent optical properties and material qualities.[1–5] Among them, β-BaB_2O_4 (BBO) and LiB_3O_5 (LBO) are the most outstanding. The SHG coefficient of BBO is reported to be three to six times larger than that of KH_2PO_4 (KDP). It has also a wide transparent and phase matchable region, good optical quality, and a high damage threshold.[1] The fundamental electronic structure and optical properties of this new nonlinear optical crystal are still not well understood, and rigorous theoretical investigation is of obvious interest.

We have previously reported the electronic structure and optical properties calculations of LBO (Ref. 6) and $KTiOPO_4$ (KTP) (Ref. 7) using the first-principles orthogonalized linear combination of atomic orbitals method (OLCAO) in the local-density approximation. KTP is another excellent nonlinear-optical crystal that has been widely studied.[8] In this paper, we report a detailed calculation for the BBO crystal and compare the result with recent experimental data using vacuum ultraviolet (VUV) spectroscopy and x-ray photoemission spectroscopy (XPS).[9] We also compare and contrast with the result for the LBO crystal.[6]

BBO crystalizes in both high- (α-BaB_2O_4) (Ref. 10) and low-temperature (β-BaB_2O_4) phases.[11] The crystal structure of the low-temperature phase has been determined by several groups.[4,12–14] It has a space group of C_{3v}^6-R_{3c}. The trigonal unit cell contains six formula units for a total of 42 atoms. The ionic group $(B_3O_6)^{-3}$ contains planar conjugated π orbitals perpendicular to the c axis which are believed to be the source of large SHG coefficients. There are two types of O atoms in the $(B_3O_6)^{-3}$ complex: the O(1) atom has two nearest-neighbor (NN) B atoms, while O(2) has only one NN B atom. The crystal structure can be viewed as consisting of alternating and closely spaced layers of $(B_3O_6)^{-3}$ and Ba^{+2} ions. The structure of LBO is quite different.[15] The orthorhombic cell contains four formula units with three nonequivalent B and five nonequivalent O sites. Two of the B atoms form threefold bonding with O, similar to that in BBO. The other B site is fourfold bonded to O in the form of a distorted tetrahedron.

We used the crystal structure determined by Fröhlich[13] for our calculation of BBO. The structure is very close to that determined earlier by Chen, Wu, and Li,[4] which has a slightly larger reported R value. The lattice structure and the interatomic distances for both the BBO and LBO crystals are summarized in Table I.

The electronic structure of β-BaB_2O_4 crystal is calculated using the first-principles self-consistent OLCAO method within the local-density approximation. The method has been applied to study the electronic properties of many complex crystals.[16] In the present calculation, the basis functions for BBO consist of atomic orbit-

0163-1829/93/48(24)/17695(8)/$06.00

als of Ba ([Xe] core plus 6*s*, 6*p*, and 5*d*, with the Ba 5*p* treated as the valence orbital), B (1*s*, 2*s*, 2*p*, 3*s*, and 3*p*), and O (1*s*, 2*s*, 2*p*, 3*s*, and 3*p*). Each atomic orbital was expressed as combinations of sixteen Gaussian-type orbitals (GTO's) with decaying exponents ranging from 50 000 to 0.15. The inclusion of excited atomic state orbitals in the basis expansion is necessary for an accurate determination of high conduction-band states involved in the optical transitions at high photon energies. Spin-orbit interactions are ignored in the present calculation. For the Ba atom, this can have some effect on the energy levels with significant Ba mixing. The crystal potential and the charge density were linearly fitted to superpositions of atom-centered functions.[16] The O(1) and O(2) atoms were treated as different atoms. We used three special **k** points in the Brillouin zone (BZ) for self-consistent iterations, and achieved a final fitting accuracy of less than 0.003 electron per valence electron in the cell. For the density of states (DOS) and linear optical calculations, 30 **k** points in the irreducible portion of the BZ were employed. Because of the large unit cell, this number of **k** points is more than adequate for a high-resolution result.

The experimental VUV spectra were taken using a laser plasma sourced vacuum ultraviolet spectrophotometer[17,18] operating from 28 to 700 nm (44–2 eV) with a resolution of 0.2–0.6 nm. The experimental reflectivities were Kramers-Kronig analyzed[19] to yield the reflected phase, and then used to calculate the complex dielectric constant. The samples were single crystals of good optical quality, and were polished using a colloidal ceria polishing method. Optical reflectivity measurements above the band gap probe a depth on the order of 50 nm, and therefore the samples were lightly polished prior to measurement to avoid any thin hydroxide or carbonate surface layers which appeared to form after long exposure to room air.

II. RESULTS

A. Band structures

The calculated band structure of BBO is shown in Fig. 1. Both the valence bands (VB's) and conduction bands (CB's) are very flat, similar to other nonlinear optical crystals such as LBO (Ref. 6) and KTP.[7] The top of the VB is at Γ, and the bottom of the CB is at X, with an indirect gap of 5.52 eV. However, the direct gaps are only slightly larger (5.57 eV at X, 5.61 eV at Γ, and 5.55 eV at a point along Γ-A). These values are to be compared with the measured optical gap of 6.43 eV.[8] For the LBO crystal, the calculated band gap of 7.37 eV is direct at Γ,[6] compared to the measured value of 7.75 eV.[3] In BBO, the upper VB region consists of five narrow bands. The topmost one has a width of about 1.4 eV which is separated from the next one by a gap of about 0.4 eV. In LBO, the upper VB region has several minigaps.[6] The

TABLE I. Comparison of structures and properties of β-BaB_2O_4 and LiB_3O_5.

Crystal	β-BaB_2O_4	LiB_3O_5
Crystal structure	trigonal	orthorhombic
Lattice const. (Å)	$a=8.38$ $\beta=96.65°$	$a=8.46$ $b=5.13$ $c=7.38$
Formula unit/cell	6	4
Space group	C_{3v}^6-R_{3c}	$Pn21a(C_{2v}^9)$
Structural units	Planer $(B_3O_6)^{-3}$	Planar threefold Tetrahedral fourfold
B-O dist. (Å)	1.329–1.415	1.368 [average for $B(1)$] 1.373 [average for $B(3)$] 1.476 [average for $B(2)$]
Band gap (eV)	5.52 (indir.) 5.61 (dir. at Γ) 5.57 (dir. at X)	7.37 (dir. at Γ)
Expt. gap (eV)	6.43	7.78
Effective Mulliken charges (electrons):		
Ba (or Li)	6.06	0.94
B	2.46	2.34
O	6.51 (O(1)) 6.70 (O(2))	6.36, 6.96

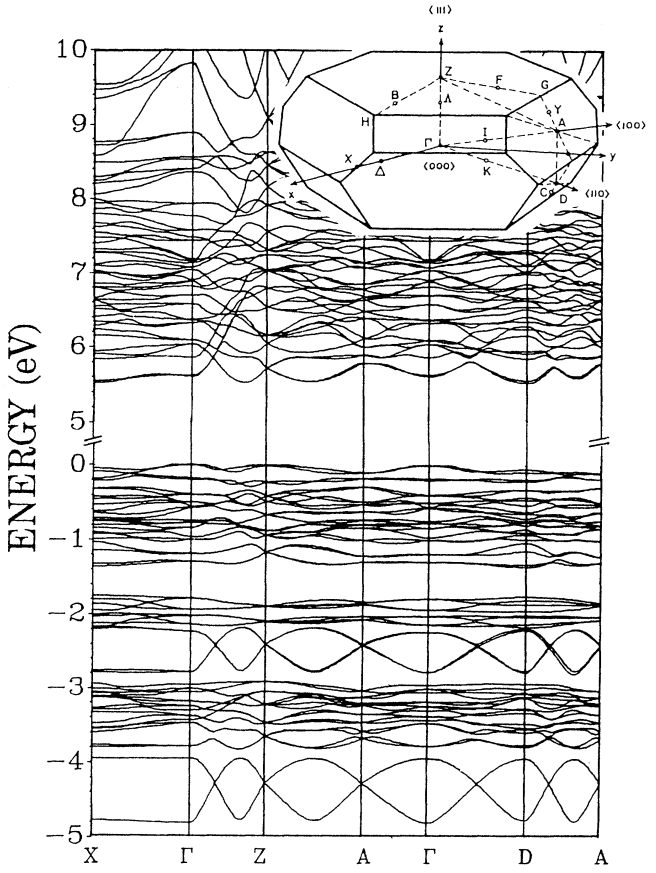

FIG. 1. Calculated band structures of β-BaB_2O_4. Inset at top shows the Brillouin zone.

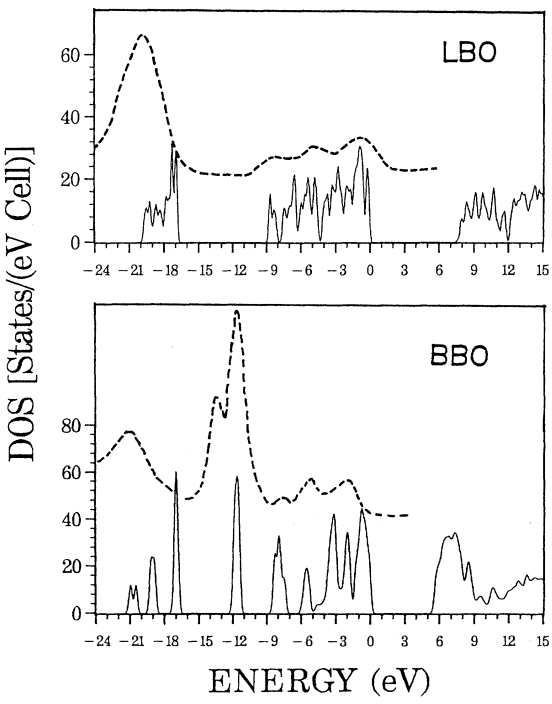

FIG. 2. Total DOS of (a) LBO and (b) BBO. The dashed lines are the experimental XPS data from Ref. 8.

bottoms of the CB's in BBO and LBO are quite different. In the BBO crystal, the CB minimum is at X with a very large electron effective mass. The CB minimum in LBO is at Γ, and has a reasonable electron effective mass of about 0.8.[6]

Hsu and Kasowski reported the calculation of the electronic and optical properties of BBO and LBO crystals using an *ab initio* pseudofunction energy-band method.[20] They obtained band gaps of 4.56 eV for BBO and 6.9 eV for LBO, both smaller than our calculated values.

B. Density of states

In Fig. 2, we display the total density of states (DOS) of both LBO and BBO crystals. Also shown are the experimental XPS data for the VB.[9] Since the resolution for the XPS spectra (0.7 eV) is quite low, only the gross features in the DOS can be compared. As can be seen from Fig. 2, the agreement between general profiles of the spectra is quite good. The major difference seems to be that the measured semi-core-like Ba 5p peak centered at -12 eV is a doublet. The doublet is related either to a surface effect or is due to spin-orbit splitting, which has not been taken into account in the calculation. Also, the calculated O 2s levels are at lower binding energy (closer to the VB top) than the measured ones in both crystals. This is also true for most of the oxides, and is related to the correlation effect of the localized nature of the O 2s states which are not well described by the LDA theory. In the upper VB region between 0 and -9.0 eV, XPS data show three broad peaks which are well reproduced by the calculation. The calculation actually suggests that the first broad peak may consist of three narrower peaks.

In Figs. 3 and 4, we show the orbital-projected partial DOS (PDOS) for Ba, B, and the two types of O, O(1) and O(2), in the BBO crystal. Since the PDOS were obtained using the Mulliken partitioning scheme,[21] which is not accurate if the basis functions involve extended orbitals such as in the present calculation, the PDOS presented here are for illustrative purpose only. Nevertheless, we can still see a substantial difference in the PDOS of O(1) and O(2) because of their different local bonding environment. The total O 2s peaks have three structures roughly at -17.0, -19.0, and -20.7 eV. The two lower peaks derive mainly from the O(1) atom, while the higher one originates exclusively from the O(2) atom. This is simply a reflection of the fact that O(1) has two B atoms as NN's, and thus a stronger interaction, and O(2) has only one B atom as a NN. For the same reason, the VB peaks at -8 and -7 eV are the result of strong hybridization between the 2p states of O(1) and a hybrid of 2s and 2p orbitals of B. For the upper three peaks in the VB at -3.8, -2.1, and -0.9 eV, the lower one at -3.8 eV can be traced to the bonding between O(2) 2p and B 2p. The other two correspond to the nonbonding orbitals of O(2) and O(1). It is not surprising to see that the strong top peak at -0.9 eV originates from O(2). O(2) has only one

B atom as a NN and therefore has a stronger nonbonding peak.

The semi-core-like Ba $5p$ peak at -11.7 eV appears to have little interaction with other orbitals. On the other hand, the two Ba $6s$ electrons are almost completely ionized since their PDOS are high in the CB region. This unique feature is important in elucidating the role played by the Ba atom in the overall bonding picture of the BBO crystal, and will be further discussed below. We also note that the bottom of the CB is mainly from the Ba $5d$ orbitals with some admixture from B $2p$. This fact is important in the discussion of optical absorption near the threshold.

C. Charge distribution

The bonding picture in the BBO and LBO crystals can be more vividly illustrated by plotting the charge-density maps of specific crystallographic planes. For a BBO crystal, we chose three planes: (1) a plane perpendicular to the **c** axis containing the planar $(B_3O_6)^{-3}$ unit; (2) a plane perpendicular to the **c** axis containing the Ba ions; and (3) a plane parallel to the **c** axis and containing some

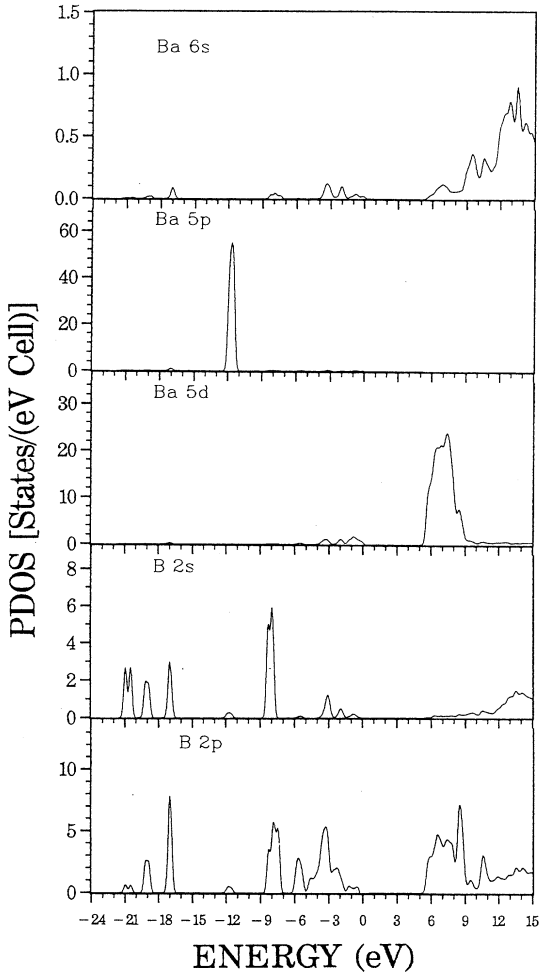

FIG. 3. Orbital-resolved partial DOS of Ba and B in β-BaB_2O_4.

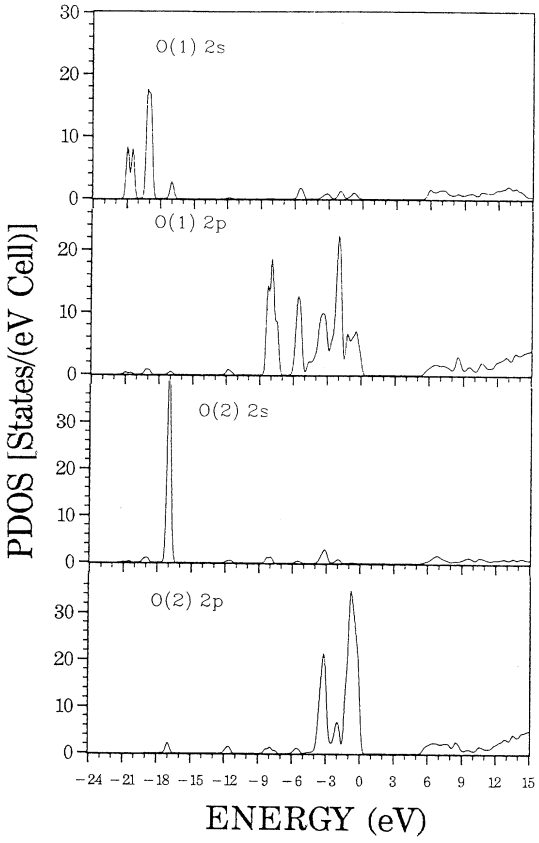

FIG. 4. Orbital-resolved partial DOS of O(1) and O(2) in β-BaB_2O_4.

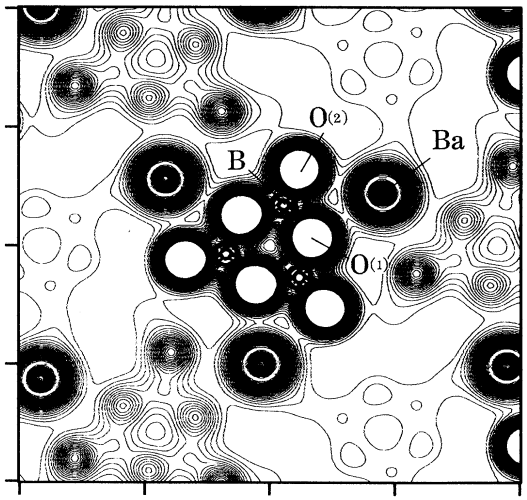

FIG. 5. Charge-density distribution in β-BaB_2O_4 on the [001] plane containing a $(B_3O_6)^{-3}$ unit (at the center). The other charges are from ions in the planes adjacent to it. The contour lines are from 0.01 to 0.25 by 0.005 all in units of electrons/(a.u.)$^{-3}$.

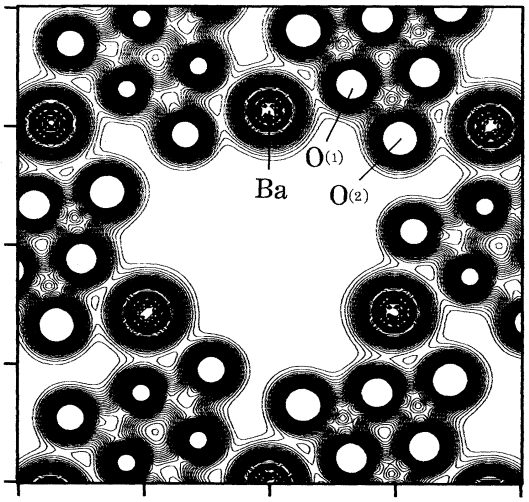

FIG. 6. Charge-density distribution in β-BaB_2O_4 on the [001] plane containing Ba atoms. The contour units are the same as Fig. 5.

Ba ions and also close to O ions. The calculated charge densities on these three planes are shown in Figs. 5, 6, and 7, respectively. Figure 5 shows the $(B_3O_6)^{-3}$ ion to be a clusterlike charge unit with a planar intracluster O-B covalent bonding. This cluster unit is bonded to the Ba atoms in the adjacent layers. The difference in the charge distribution between O(1) and O(2) due to different numbers of NN B atoms is quite clear. The degrees of distortion of the O charge from that of a spherical symmetry are quite obvious. Figure 6 shows the charge distribution in the Ba plane, which also shows the charges of the $(B_3O_6)^{-3}$ units from the planes above and below it. Most conspicuous is the nearly empty region in the middle of the quasitriangular array of Ba ions. As alluded to earlier, the near-complete donation of the two Ba-6s electrons to the $(B_3O_6)^{-3}$ unit is the logical explanation. However, because of the large orbital radius of the semicore-like Ba 5p orbital, the bonding between Ba and O atoms in the $(B_3O_6)^{-3}$ unit in the adjacent planes has a certain degree of covalent character. This partly covalent and partly ionic bonding between Ba and O atoms is ultimately responsible for a three-dimensional network structure in the BBO crystal. This networklike charge distribution which links ions in different planes is more clearly illustrated in Fig. 7, which also reveals zigzag open channels along the z direction.

Similar charge-density maps for the LBO crystal are shown in Figs. 8 and 9. LBO has an orthorhombic cell with a networklike structure. Figure 8 shows a plane containing three B atoms in the $(B_3O_7)^{-5}$ unit, and shows the bonding pattern between B and O. Two of the B atoms with a planar bonding to O are quite similar to the $(B_3O_6)^{-3}$ unit in a BBO crystal; the other B atom has four NN O atoms in a tetrahedral configuration and a longer B-O bond length. Two of the O atoms are close to the plane of Fig. 8, the other two are above and below the plane. Figure 9 shows the charge distribution in the **a**-**c** plane with $y=0$. A similar map of the $y=b/2$ plane (not shown) shows a 180° rotational symmetry. These two symmetry-related planes have Li, B, and O atoms very close to them. It is quite evident that the charge distribution in LBO consists of linked ions in a network-type structure similar to BBO. However, in contrast to BBO, there is no clear layered structure of molecular arrangement, and this may account for the difference in the electronic structures of these two crystals. In LBO, the Li atom is in the spacious location of the network, and gives up almost all its valence charge, yet it does not have a large semi-core-like orbital to participate in a partially covalent type of bonding.

The effective charges on different ions as calculated by the Mulliken scheme are summarized in Table I.

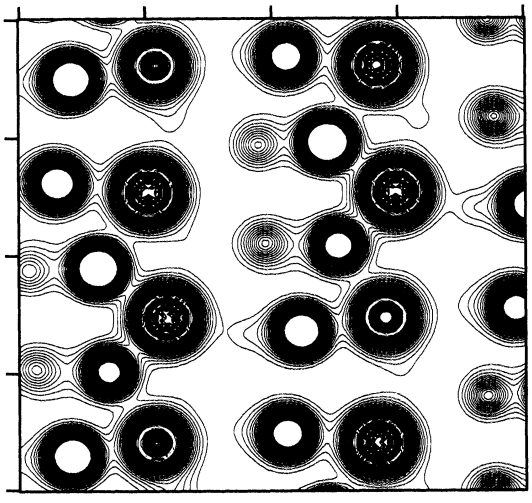

FIG. 7. Charge-density distribution in β-BaB_2O_4 in a plane parallel to the **c** axis. The contour units are the same as Fig. 5. Note that only five of the Ba ions in this diagram are strictly in the plane.

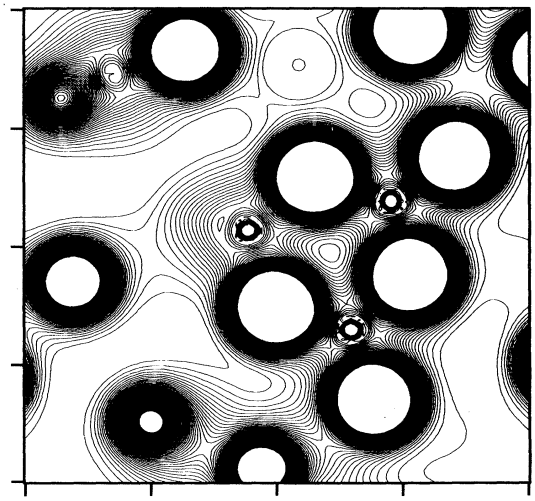

FIG. 8. Charge-density distribution in LiB_3O_5 in a plane containing three B atoms in the $(B_3O_7)^{-5}$ unit. The contour unit is the same as Fig. 5.

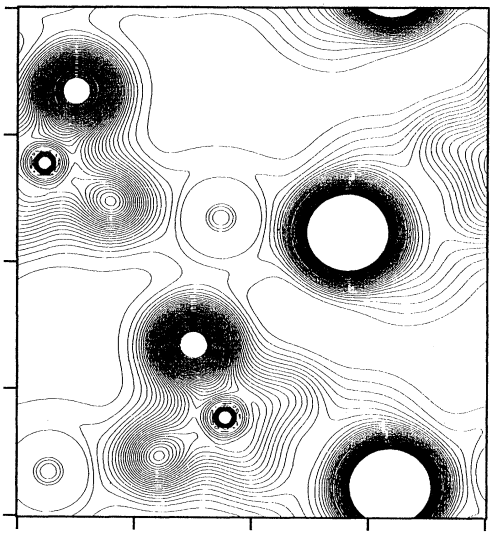

FIG. 9. Charge-density distribution in LiB_3O_5 in the **a-c** plane with $y=0$.

D. Optical properties

Based on the calculated band structure, the linear optical properties of the BBO crystal were calculated. The energy eigenvalues and wave functions at 30 **k** points in $\frac{1}{12}$th of the Brillouin zone were used to evaluate the momentum matrix elements of optical transitions. The diagonal conductivity tensor elements were evaluated according to

$$\sigma_{xx}(E)=\frac{2\pi e^2}{mE\Omega}\frac{\Omega}{(2\pi)}3\int d\mathbf{k}\sum_{n,l}|\langle\psi_n(\mathbf{k},\mathbf{r})|\mathbf{P}_x|\psi_l(\mathbf{k},\mathbf{r})\rangle|^2 \times f_l(\mathbf{k})[1-f_n(\mathbf{k})] \times\delta[E_n(\mathbf{k})-E_l(\mathbf{k})-E]\,, \quad (1)$$

where $E=\hbar\omega$ is the phonon energy, Ω is the cell volume, and $f_l(\mathbf{k})$ the Fermi distribution function. From the frequency-dependent optical conductivity curve, all other optical functions can be easily obtained,[16] subject only to errors introduced in the Kramers-Kronig conversion between the real and imaginary components of the optical constants.

Figure 10 shows the calculated imaginary parts of the dielectric function for the LBO and BBO crystals. Also shown are the imaginary dielectric constants determined from the VUV reflectivity measurement for photon energies up to 40 eV. It should be pointed out that in Fig. 10, there is no shift in energy scale either in the experimental or theoretical curve in order to align the position of the absorption peaks. As can be seen from Fig. 10, there is good agreement on the general profiles of the calculated and measured spectra. However, the locations of some of the absorption structures in the experimental curves are not sufficiently well reproduced by the calculation. The major discrepancies seem to be the position of the deep valley near 12.5 eV in the LBO crystal, and the additional absorption structure near 7 eV above the threshold in the BBO crystal. Since we believe the calculation has been performed with reasonable accuracy within the context of the one-electron local-density theory, either the experimental sample contains some defects which affect the optical spectra, or the LDA theory has some deficiency in adequately representing the unoccupied conduction-band states. Of course, possible after effects of neglecting spin-orbit coupling or inadequacy in the basis set should not be ruled out. We should perhaps point out that similar OLCAO-LDA calculations on less complicated oxides such as α quartz,[22] α-Al_2O_3 and MgO,[23] and $BaTiO_3$ (Ref. 24) have results in quite good agreement with similar VUV measurements. The peak seen in BBO at ~22 eV is identical to one seen in $BaTiO_3$ at ~20 eV, and it must be due to the transaction from the filled Ba^{2+} $5p$ band at -12 eV to about 10 eV above the VB. Since Li has no p electrons there are no transitions seen in a comparable energy range in LBO crystal.

In the insets of Fig. 10, we show the calculated conductivity curves near the threshold for both crystals. Also shown are the experimental absorption curves.[8] It is apparent that in this frequency region, the agreement between experiment and calculation is excellent. The positions of the calculated edges differ from the experimental ones by only about 0.2 eV.

Figure 11 shows the real part of the linear dielectric function $\varepsilon_1(\omega)$ obtained from the Kramers-Kronig transformation of the imaginary part. To investigate the opti-

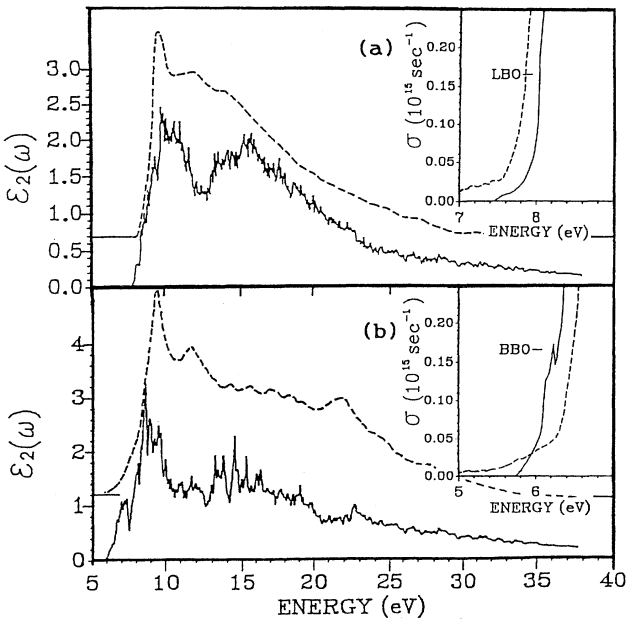

FIG. 10. Calculated imaginary part of the dielectric function, $\varepsilon_2(\omega)$: (a) LBO crystal; (b) BBO crystal. The dashed lines are the experimental VUV data. Insets: calculated optical conductivities of LBO and BBO near the threshold with no shift in energy. The dashed lines are the experimental absorption data from Ref. 8.

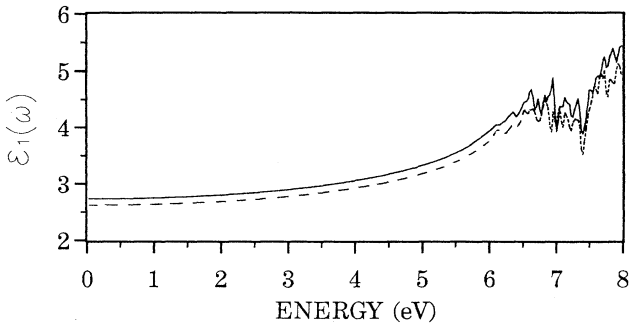

FIG. 11. The calculated real part of the dielectric function $\varepsilon_1(\omega)$ of BBO. Solid line, in-plane component averaged over the x and y directions; dashed line, z component parallel to the c axis.

cal anisotropy in the BBO crystal, the $\varepsilon_1(\omega)$ curve is resolved into two components, one parallel to the c axis and the other perpendicular to it. The parallel component has a slightly lower value, and this is in agreement with the refractive index measurement of Chen *et al.*[12] The static dielectric constant at zero frequency $\varepsilon(0)$ averaged over three directions is 2.72 for BBO, close to the value of 2.70 for LBO.[3] The refractive index measurement by Chen *et al.*[2] shows $\varepsilon(0)=n^2$ to be 1.96 and 1.69 for the two polarization directions. This indicates that the measured optical anisotropy is much larger than the calculated one. It could mean that some aspects of the theoretical calculation may not be adequate. The calculated components of the static dielectric constants of BBO and LBO together with the measured data are listed in Table II.

TABLE II. Comparison of calculated dielectric constants of β-BaB_2O_4 and LiB_3O_5. Measured values are in parentheses.

	β-BaB_2O_4	LiB_3O_5
$\varepsilon(0)$	2.72	2.70
$\varepsilon_x(0)$	2.82 (2.74[a])	2.57 (2.45[b])
$\varepsilon_y(0)$	2.66	2.72 (2.53[b])
$\varepsilon_z(0)$	2.70 (2.38[a])	2.81 (2.58[b])

[a]Reference 2 at $\lambda=1079$ nm.
[b]Reference 3 at $\lambda=1064$ nm.

III. CONCLUSION

We have calculated the band structure of the BBO crystal using a first-principles method, and compared it with experimentally determined interband transitions. The result shows some marked differences from another nonlinear-optical crystal LBO, because of their difference in the local bonding structures. The presence of two different types of O atoms in the $(B_3O_6)^{-3}$ unit, the unique role played by the Ba $5p$ orbital in bonding with O, and the planer layered structure of the crystal, all contribute to the unique electronic properties of the BBO crystal.

There are some common features in the calculated electronic and optical properties of the three nonlinear optical crystals BBO, LBO, and KTP. First, the calculated band gaps are rather close to the measured optical gaps. This is contrary to the conventional belief that LDA theory generally underestimates the band gap for insulators. Second, all three crystals have rather sharp absorption edges where no excitonic levels have been detected. Third, there is considerable optical anisotropy in all three crystals near the absorption edges. We conjecture that the anisotropies in the layered $(B_3O_6)^{-3}$ structure and the linear-optical properties are probably responsible for its large nonlinear optical coefficient in BBO. This is different from the LBO or KTP crystal. In the KTP crystal, the excellent nonlinear-optical properties are believed to be due to the presence of a short Ti-O bond in the TiO_6 octahedral unit, and the fact that the bottom of the CB in KTP is dominated by Ti $3d$ states.[7] In the LBO crystal, the nonlinearity is believed to originate from the two different B-O bonding configurations in the $(B_3O_7)^{-5}$ unit, one planar and the other tetrahedral. It will be highly desirable to calculate the nonlinear-optical parameters from first-principles band-structure results, and to ascertain if the origin of large optical nonlinearity can accurately be traced. Calculations of second- and third-harmonic generations in simple cubic semiconductors has been successfully carried out by us.[25–27] It is hoped that similar calculations can be extended to complex nonlinear optical crystals such as LBO and BBO. At present, theoretical investigation of the nonlinear-optical properties of complex inorganic crystals has almost concentrated on quantum chemical methods in which a basic molecular (or ionic) unit has to be identified.[1] The present study shows that such an approach may be oversimplified, and that the band-structure method will be a more fundamental approach that can be universally applied to all types of crystals.

ACKNOWLEDGMENTS

This work was supported by the Office of Naval Research under Grant No. N00014-91-J-1110. The authors would like to acknowledge Dr. Chuang-tian Chen for supplying the BBO and LBO crystals studied experimentally.

[1]C.-t. Chen and G.-Z. Liu, Ann. Rev. Mater. Sci. **16**, 203 (1986), and references cited therein.
[2]C. T. Chen, B. C. Wu, A. D. Jiang, and G. M. You, Sci. Sinica Ser. **12**, 235 (1985).
[3]Chuangtian Chen *et al.*, J. Opt. Soc. Am. B **6**, 616 (1989).
[4]Chuangtian Chen, Y. Wu, and R. Li, J. Cryst. Growth **99**, 790 (1990).
[5]Y. Wu, T. Sasaki, S. Nakai, A. Yokotani, H. Tang, and Chuangtian Chen, Appl. Phys. Lett. **62**, 2614 (1993).
[6]Y.-N. Xu and W. Y. Ching, Phys. Rev. B **41**, 5471 (1990).
[7]W. Y. Ching and Y.-N. Xu, Phys. Rev. B **44**, 5332 (1991).
[8]J. D. Bierlein and H. Vanherzeele, J. Opt. Soc. Am. B **6**, 622 (1989).
[9]R. H. French, J. W. Ling, F. S. Ohuchi, and C. T. Chen, Phys.

Rev. B **44**, 8496 (1991).
[10]A. D. Mighell, A. Perloff, and S. Block, Acta Crystallogr. **20**, 819 (1966).
[11]K. H. Hübner, in *Nelles Jahrb Mineral. Manalsh,* p. 335 (1969).
[12]J. Liebertz and S. Stahr, Z. Kristallogr. Kristallgeom. Krystallphys. Kristallchem. **165**, 91 (1983).
[13]R. Fröhlich, Z. Kristallogr. Kristallgeom. Krystallphys. Kristallchem. **168**, 109 (1984).
[14]Lu Shao-Fang, Ho Mei-Yun, and Huang Jin-Linhg, Acta Phys. Sin. **31**, 948 (1982).
[15]H. von Konig and R. Hoppe, Z. Anorg. Allg. Chem. **439**, 71 (1978).
[16]W. Y. Ching, J. Am. Ceram. Soc. **73**, 3155 (1991).
[17]M. L. Bortz and R. H. French, Appl. Phys. Lett. **5519**, 1955 (1989).
[18]R. H. French, Phys. Scr. **41**, 404 (1990).
[19]M. L. Bortz and R. H. French, Appl. Spectrosc. **43**, 1498 (1989).
[20]W. Y. Hsu and R. V. Kasowski, Bull. Am. Phys. Soc. **37**, 547 (1992).
[21]R. S. Mulliken, J. Am. Chem. Soc. **23**, 1833 (1955).
[22]Y.-N. Xu and W. Y. Ching, Phys. Rev. B **43**, 4461 (1991).
[23]Y.-N. Xu and W. Y. Ching, Phys. Rev. B **44**, 11 048 (1991).
[24]Y.-N. Xu, W. Y. Ching, and R. H. French, Ferroelectrics **111**, 23 (1990).
[25]M.-Z. Huang and W. Y. Ching, Phys. Rev. B **45**, 8738 (1992).
[26]M.-Z. Huang and W. Y. Ching, Phys. Rev. B **47**, 9464 (1993).
[27]W. Y. Ching and M.-Z. Huang, Phys. Rev. B **47** 9479 (1993).